Diagnostic Immunohistochemistry for Soft Tissue and Bone Tumors: An Update

Inga-Marie Schaefer, MD and Jason L. Hornick, MD, PhD

Abstract: Although some soft tissue and bone tumors can be identified based on histologic features alone, immunohistochemistry plays a critical diagnostic role for most mesenchymal tumor types. The discovery of recurrent genomic alterations in many benign and malignant mesenchymal neoplasms has added important biologic insights and expanded the spectrum of some diagnostic subgroups. Some tumors are defined by unique genomic alterations, whereas others share abnormalities that are not tumor-specific and can be observed in a sometimes broad range of biologically unrelated neoplasms. We herein focus on novel immunohistochemical markers, based on molecular genetic alterations, which are particularly useful in the diagnostic workup of selected groups of soft tissue and bone tumors, including recently described entities, specifically round cell sarcomas (Ewing sarcoma, *CIC*-rearranged sarcoma, and *BCOR*-rearranged sarcoma), vascular tumors (epithelioid hemangioma, epithelioid hemangioendothelioma, and pseudomyogenic hemangioendothelioma), SMARCB1-deficient neoplasms, adipocytic tumors (spindle cell/pleomorphic lipoma, atypical spindle cell lipomatous tumor, and conventional atypical lipomatous tumor), giant cell-rich bone tumors (giant cell tumor of bone and chondroblastoma), and biphenotypic sinonasal sarcoma. Given the complex nature of sarcoma classification, and the rarity of many mesenchymal tumor types, careful integration of clinical presentation, imaging features, histology, immunophenotype, and cytogenetic/molecular alterations is crucial for accurate diagnosis of soft tissue and bone tumors.

Key Words: sarcoma, CAMTA1, FOSB, SMARCB1, PAX3, histone 3

(*Adv Anat Pathol* 2018;00:000–000)

The rarity and yet striking biologic diversity of soft tissue and bone tumors make the diagnostic workup of this group of tumors challenging. Substantial advances in recent years have provided important insights into the genomic underpinnings of many benign and malignant mesenchymal neoplasms and led to the gradual incorporation of immunohistochemistry, cytogenetic, and molecular genetic techniques into routine diagnostics. We herein focus on the most recent advances that have been made in selected groups of soft tissue and bone tumors and highlight important immunohistochemical findings that aid in their diagnostic workup—in correlation with clinical presentation, morphologic features, and genomic alterations.

As notable examples, newly emerging entities in the group of round cell sarcomas and vascular tumors can now be distinguished by the expression of markers that are directly or indirectly linked to the underlying defining cytogenic alteration. The identification of distinct cytogenetic features in subsets of vascular tumors in the past few years has led to the introduction of associated immunohistochemical markers that directly reflect the underlying genetic aberration.

In contrast, the spectrum of benign and malignant mesenchymal (and epithelial) neoplasms that share SMARCB1 deficiency continues to expand, which may lead to diagnostic challenges in tumors with otherwise similar morphologic and immunophenotypic characteristics and yet marked differences in biologic behavior, such as epithelioid schwannoma and epithelioid malignant peripheral nerve sheath tumor (MPNST). In addition, the recently refined classification of adipocytic tumors recognizes atypical spindle cell lipomatous tumor as a distinct entity, thereby expanding the spectrum of adipocytic neoplasms with spindle cell features. The discovery of highly recurrent mutations in histone 3.3 encoding genes in certain giant cell-rich bone tumors led to the introduction of mutation-specific antibodies with high specificity and sensitivity, which directly point to the underlying type of mutation. Finally, biphenotypic sinonasal sarcoma represents a recently described entity defined by distinct cytogenetic aberrations with direct immunohistochemical correlates. Recent advances in the immunohistochemical workup and underlying genetic alterations of these groups of soft tissue and bone tumors are summarized in Table 1.

The increasing use of next-generation sequencing and improved bioinformatics algorithms for structural variant detection in the diagnostic workup of soft tissue and bone tumors has substantially contributed to the field, and is expected to continue to identify novel entities and introduce more nuances into existing classification systems. However, with the increasing discovery of novel molecular and cytogenetic findings of unknown biologic significance, critical correlation with morphologic and immunohistochemical features remains of critical importance in the diagnostic workup of mesenchymal neoplasms.

EMERGING ENTITIES IN THE GROUP OF ROUND CELL SARCOMAS

While Ewing sarcoma represents the prototypical round cell sarcoma, the recent discovery of recurrent cytogenetic alterations in round cell sarcomas lacking *EWSR1* rearrangement has refined the diagnostic spectrum of round cell sarcomas (Table 1). Specifically, round cell sarcomas harboring rearrangements of *CIC* or *BCOR* will be discussed herein.

Ewing Sarcoma

Ewing sarcoma is comprised of poorly differentiated, primitive cells with round nuclei, inconspicuous nucleoli and scant cytoplasm with a sheet-like growth pattern (Fig. 1A). The tumor cells usually display a strikingly monotonous appearance; pleomorphism is absent. However, a variety of

From the Department of Pathology, Brigham and Women's Hospital, Harvard Medical School, Boston, MA.
The authors have no funding or conflicts of interest to disclose.
Reprints: Jason L. Hornick, MD, PhD, Department of Pathology, Brigham and Women's Hospital, 75 Francis Street, Boston, MA 02115 (e-mail: jhornick@bwh.harvard.edu).

TABLE 1. Overview of Immunohistochemical Markers and Molecular Correlates in the Differential Diagnosis of Selected Round Cell Sarcomas, Vascular Tumors, SMARCB1-deficient Neoplasms, Adipocytic Tumors, Giant Cell-rich Bone Tumors, and Biphenotypic Sinonasal Sarcoma

		Immunohistochemistry		
Diagnostic Group	**Tumor Type**	**Positive Markers**	**Negative Markers**	**Genetic Alteration**
Round cell sarcomas	Ewing sarcoma	CD99 (100%), NKX2.2 (>90%)	ETV4, WT1, BCOR, CCNB3	*EWSR1-FLI1* fusion (*EWSR1-ERG*, others)
	CIC-rearranged sarcoma	CD99 (20%), ETV4 (>90%), WT1 (>90%)	NKX2.2	*CIC-DUX4* fusion (*CIC-FOXO4*)
	BCOR-rearranged sarcoma	CD99 (80%), BCOR (>90%), CCNB3 (90%)	NKX2.2	*BCOR-CCNB3* fusion (*BCOR-MAML3, ZC3H7B-BCOR7, KMT2D-BCOR*)
Vascular tumors	Epithelioid hemangioma	CD31, ERG, FOSB (50%)	—	*ZFP36-FOSB* fusion, *WWTR1-FOSB* fusion, *FOS* rearrangement
	Epithelioid hemangioendothelioma	CD31, ERG, keratin (25%), CAMTA1 (90%), TFE3 (5%)	—	*WWTR1-CAMTA1* fusion (90%), *YAP1-TFE3* fusion (5%)
	Pseudomyogenic hemangioendothelioma	CD31, ERG, keratin, FOSB (>90%)	—	*SERPINE1-FOSB* fusion
SMARCB1-deficient tumors	Malignant rhabdoid tumor	Keratin, EMA, various others	SMARCB1 (100%)	*SMARCB1* mutation/deletion
	Epithelioid sarcoma	Keratin, EMA, CD34 (55%)	SMARCB1 (90%)	*SMARCB1* deletion (miR-206,-381, 671-5p upregulation)
	Epithelioid schwannoma	S100 (100%), SOX10 (100%), GFAP (40%)	SMARCB1 (40%)	NA
	Epithelioid MPNST	S100 (100%), SOX10 (100%), GFAP (60%)	SMARCB1 (70%)	NA
	Poorly differentiated chordoma	Brachyury (100%), keratin (100%)	SMARCB1 (100%)	NA
	Myoepithelial carcinoma	Myoepithelial markers (p63, SMA, GFAP, S100), keratin	SMARCB1 (10-40%)	NA
	Extraskeletal myxoid chondrosarcoma	S100 (<50%), EMA (30%)	SMARCB1 (17%)	*NR4A3-EWSR1* fusion (*NR4A3-TAF15*)
	Renal medullary carcinoma	PAX8, keratin	SMARCB1 (90%)	*SMARCB1* rearrangement
Adipocytic tumors with spindle cell features	Spindle cell/pleomorphic lipoma	CD34	RB1	13q14 deletion (*RB1*)
	Atypical spindle cell lipomatous tumor	CD34 (60%), S100 (40%), desmin (20%)	RB1 (50%)	13q14 deletion (*RB1*)
	Atypical lipomatous tumor	MDM2, CDK4, HMGA2	—	12q13-15 high-level amplification (*MDM2*, *CDK4*, *HMGA2*)
Giant cell-rich bone tumors	Giant cell tumor of bone	H3G34W (>90%, rarely G34V or G34R)	H3K36M	*H3F3A* (*H3F3B*) G34W mutation (G34V, G34R, G34L, G34M)
	Chondroblastoma	H3K36M (>95%)	H3G34W	*H3F3B* (*H3F3A*) K36M mutation
Sinonasal sarcoma	Biphenotypic sinonasal sarcoma	S100, SMA (desmin, myogenin), PAX3 (PAX8), β-catenin (TLE1)	—	*PAX3-MAML3* fusion (*PAX3-FOXO1*, *PAX3-NCOA1*, others)

EMA indicates epithelial membrane antigen; GFAP, glial fibrillary acidic protein; MPNST, malignant peripheral nerve sheath tumor; NA, not available.

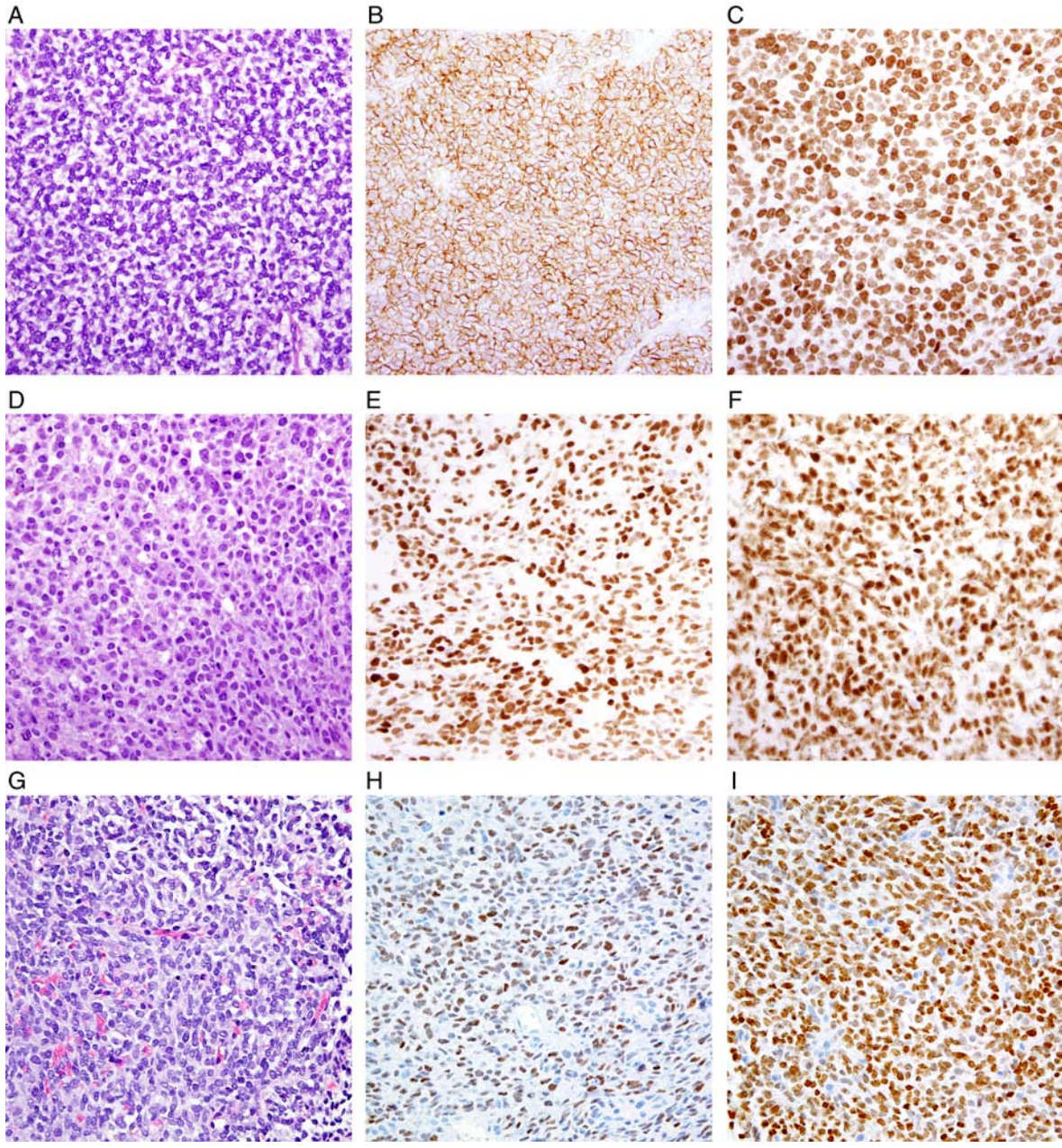

FIGURE 1. Emerging entities in the group of round cell sarcomas. Ewing sarcoma is characterized by sheets of uniform tumor cells with rounded nuclei and inconspicuous nucleoli (A) with diffuse membranous expression of CD99 (B) and nuclear expression of the transcription factor NKX2.2 (C). *CIC*-rearranged sarcoma is comprised of a morphologically more heterogeneous population of primitive round to ovoid or spindled tumor cells (D) with nuclear expression of ETV4 (E) and WT1 (F). *BCOR*-rearranged sarcoma features primitive appearing round to ovoid and occasionally spindled tumor cells, arranged in fascicles or showing a patternless architecture with variably prominent myxoid stroma (G). These tumors show expression of BCOR (H) and CCNB3 (I) in most cases.

rare morphologic variants has been described.[1] Approximately 90% of Ewing sarcomas harbor t(11;22)(q24;q12) leading to *EWSR1-FLI1* fusion. The remainder of cases show *EWSR1* rearrangement with other fusion partners or unknown genes.

Ewing sarcoma typically shows strong and diffuse membranous expression of CD99 (Fig. 1B), which is generally not observed to this extent in other neoplasms; this pattern is therefore relatively specific. As shown recently, nuclear expression of the transcription factor NKX2.2 is found in around 95% of Ewing sarcomas (Fig. 1C), but is also expressed in a subset of histologic mimics such as mesenchymal chondrosarcoma (in 75% of cases) and is therefore not specific for Ewing sarcoma.[2] However, the combination of CD99 and NKX2.2 is diagnostically useful.[3,4]

CIC-rearranged Sarcoma

In recent years, a novel subset of round cell sarcomas was identified that lacked *EWSR1* rearrangement and instead harbored recurrent *CIC* rearrangement, with

CIC-DUX4 fusion resulting from t(4;19)(q35;q13) or t(10;19)(q26;q13) as the most common aberration, followed by rare alternate *CIC-FOXO4* fusion.[5–7] *CIC*-rearranged sarcomas were subsequently shown to exhibit distinct transcriptional and immunohistochemical profiles that set them apart from Ewing sarcoma and further support their classification as a separate entity.[8]

CIC-rearranged sarcoma shows a predilection for the soft tissues of the trunk and extremities of young adults with a mean age of 32 years and a slight male predominance.[9] Histologically, *CIC*-rearranged sarcoma displays a higher degree of nuclear heterogeneity than observed in Ewing sarcoma, including irregular nuclear contours, variation in nuclear size, and prominent nucleoli, as well as more abundant palely eosinophilic cytoplasm, frequent mitoses, and necrosis (Fig. 1D). Expression of CD99 is variable but usually more limited in extent, being diffusely positive in only 20% of cases. In contrast to Ewing sarcoma, *CIC*-rearranged sarcomas exhibit diffuse nuclear expression of ETV4 (Fig. 1E) and WT1 (using the conventional monoclonal antibodies directed against the N-terminus of the protein; Fig. 1F) in >90% of cases. Staining for NKX2.2 is negative in the majority of cases. Of note, *CIC*-rearranged sarcoma behaves more aggressively than Ewing sarcoma, with overall survival rates of 43% versus 77%, and shows worse response to Ewing sarcoma–based chemotherapy regimens.[9] The distinction of *CIC*-rearranged sarcoma from Ewing sarcoma therefore significantly impacts prognostication.

BCOR-rearranged Sarcoma

Another subset of round cell sarcomas lacking *EWSR1* and *CIC* rearrangements was recently identified to harbor recurrent *BCOR* rearrangement, including *BCOR-CCNB3* fusion resulting from inv(X)(p11) in most cases,[10] and rare alternate rearrangement with *MAML3*, *ZC3H7B*[8] or *KMT2D*, as well as *BCOR* internal tandem duplication.[11] *BCOR*-rearranged sarcomas arise most frequently in bone and soft tissue of children with a mean age of 13 to 15 years and are more common in male patients.[11,12] Histologically, *BCOR*-rearranged sarcomas are variably cellular and are often comprised of an admixture of round and spindled cells with monomorphic nuclei embedded in a myxoid or collagenous stroma (Fig. 1G). The tumor cells show variable expression of CD99, and positive staining for BCOR[13] (Fig. 1H) and CCNB3[12] (Fig. 1I) in >90% of cases. Staining for NKX2.2 is negative. Of note, BCOR and CCNB3 immunohistochemistry is generally negative in Ewing sarcoma.[11]

The 5-year overall survival rates of *BCOR*-rearranged sarcomas are 72% to 77% and are comparable with Ewing sarcoma but significantly better than survival rates reported for *CIC-DUX4* sarcomas (see above).[11,12] *BCOR*-rearranged sarcoma has been shown to harbor transcriptional profiles distinct from Ewing sarcoma and *CIC*-rearranged sarcoma, further supporting its recognition as a separate entity.[11]

IMMUNOHISTOCHEMICAL CORRELATES OF RECURRENT CYTOGENETIC ALTERATIONS IN VASCULAR TUMORS

The discovery of recurrent cytogenetic alterations in select epithelioid (and spindle cell) vascular tumors, including epithelioid hemangioma, epithelioid hemangioendothelioma, and pseudomyogenic hemangioendothelioma, have provided insights into the genetic underpinnings of these neoplasms and have led to a more refined classification system in recent years (Table 1). For these distinctive vascular neoplasms, novel immunohistochemical markers that closely reflect underlying genetic alterations have subsequently been introduced into surgical pathology practice.

Epithelioid Hemangioendothelioma

Classified as a low-grade malignant vascular tumor, epithelioid hemangioendothelioma often arises in association with a large vein and is commonly found in soft tissues of the limbs and trunk but also occurs in lung, liver, and bone, where the tumor is often multifocal.[14] Local recurrences have been reported in 15% of cases and distant metastases in 30% of cases. Histologically, epithelioid hemangioendothelioma is characterized by a variably cellular proliferation of epithelioid endothelial cells with palely eosinophilic to glassy cytoplasm and intracytoplasmic vacuoles, arranged in cords and strands, embedded in a characteristic myxoid to hyalinized or collagenous stroma (Fig. 2A). Vascular markers such as CD31 and ERG are generally expressed by the tumor cells, and a subset of cases show positive staining for keratins. Until recently, specific immunohistochemical markers did not exist and the differential diagnosis of epithelioid hemangioendothelioma—which includes a broad range of epithelioid mesenchymal tumors and even carcinomas—was challenging in certain instances, such as highly cellular examples. However, the identification of a recurrent t(1;3)(p36.3;q25)[15] leading to *WWTR1-CAMTA1* fusion in 90% of cases,[16,17] prompted the introduction of CAMTA1 immunohistochemistry, which demonstrates diffuse nuclear expression in most cases and is highly sensitive and specific for the diagnosis of epithelioid hemangioendothelioma (Fig. 2B).[18]

Approximately 5% of cases lack *WWTR1-CAMTA1* fusion and instead harbor alternate t(X;11)(p11;q22), resulting in *YAP1-TFE3* fusion.[19] This subset of epithelioid hemangioendothelioma is characterized by distinct morphologic features and displays more abundant eosinophilic cytoplasm and sometimes prominent vasoformative features (Fig. 2C). Immunohistochemical staining for CAMTA1 is negative in these tumors, which instead show diffuse nuclear staining for TFE3 (Fig. 2D).[18]

Future studies will show whether these tumors belong to the spectrum of epithelioid hemangioendothelioma or warrant separate classification.

Pseudomyogenic Hemangioendothelioma

A vascular tumor of intermediate biological potential, pseudomyogenic hemangioendothelioma characteristically presents with multiple synchronous tumors that involve multiple tissue planes in one anatomic region and most commonly affects young to middle-aged male patients.[20] Pseudomyogenic hemangioendothelioma is associated with a low risk for distant metastasis. Histologically, the tumor is comprised of plump spindled and epithelioid cells with prominent eosinophilic cytoplasm and scattered cells with rhabdomyoblast-like cytomorphology arranged in fascicles, often accompanied by neutrophil infiltrates (Fig. 2E). Immunohistochemical staining reveals expression of vascular markers such as CD31 and ERG as well as keratins. A recently discovered recurrent t(7;19)(q22;q13), leading to

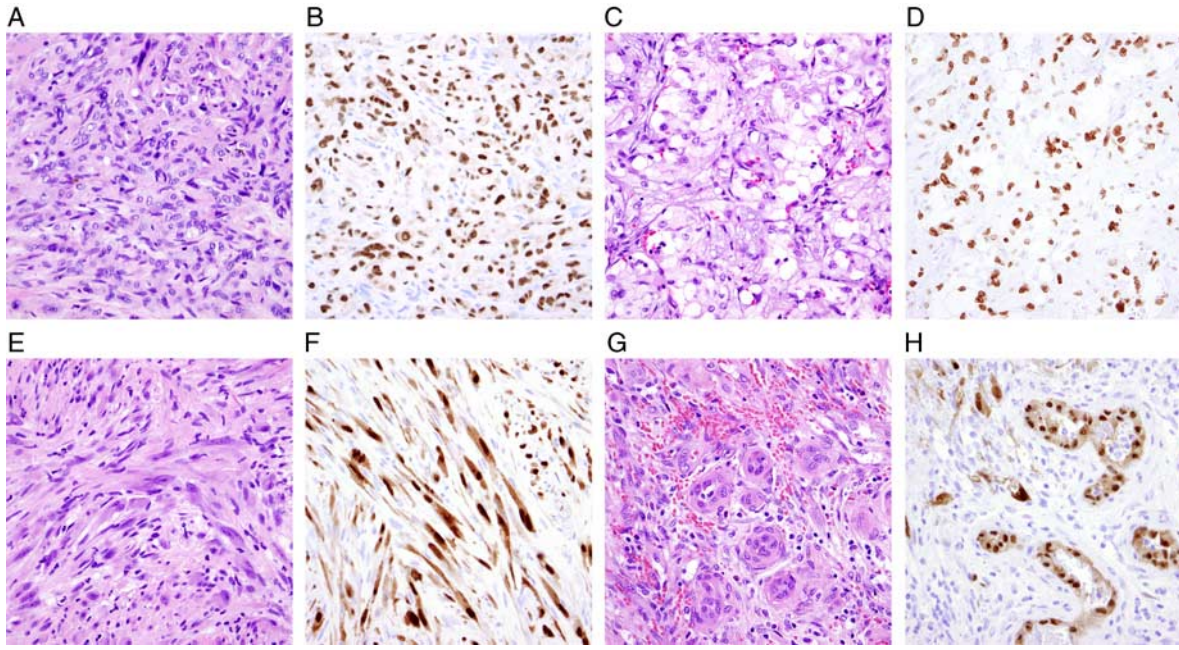

FIGURE 2. Immunohistochemical correlates of recurrent cytogenetic alterations in vascular tumors. Epithelioid hemangioendothelioma is comprised of cords and strands of epithelioid endothelial cells with palely eosinophilic to glassy cytoplasm and intracytoplasmic vacuoles, which are embedded in a myxohyaline stroma (A). Most cases show nuclear expression of CAMTA1 (B) resulting from *WWTR1-CAMTA1* fusion. A small subset of epithelioid hemangioendotheliomas with more abundant eosinophilic cytoplasm and prominent vasoformative features (C) harbors alternate *YAP1-TFE3* fusion leading to nuclear TFE3 expression (D). Pseudomyogenic hemangioendothelioma is characterized by plump spindled and epithelioid cells with prominent eosinophilic cytoplasm and occasional rhabdomyoblast-like cells arranged in fascicles (E). The tumor cells show nuclear expression of FOSB in most cases (F), resulting from *SERPINE1-FOSB* fusion. Epithelioid hemangioma exhibits prominent epithelioid endothelial cells (G). A subset of predominantly cellular epithelioid hemangiomas harbors *ZFP36-FOSB* or *WWTR1-FOSB* fusion, leading to FOSB expression (H).

SERPINE-FOSB fusion, is a defining feature of pseudomyogenic hemangioendothelioma and detected in the majority of cases.[21] Consequent FOSB expression is demonstrated by immunohistochemistry in >90% of cases; this is a useful diagnostic marker. However, FOSB expression is not specific for pseudomyogenic hemangioendothelioma and can also be observed in some epithelioid hemangiomas (see below).[22]

Epithelioid Hemangioma

Epithelioid hemangioma is a benign vascular tumor that commonly occurs in the head neck region, trunk, limbs, and deep soft tissues of middle-aged adults. Sometimes arising in association with a blood vessel, epithelioid hemangioma usually appears as a well-circumscribed and lobular mass. Histologically, the tumor is comprised of epithelioid endothelial cells with hobnail features (Fig. 2G) and a distinctive zonation of well-formed vessels at the periphery of the lesion and more compressed vessels in the center. Nuclear atypia is usually absent or mild, mitoses are rare, and nuclear pleomorphism is uncommon. Although around 20% of cases are multifocal at presentation and local recurrence is observed in 30% of cases, epithelioid hemangiomas do not metastasize.

A subset of epithelioid hemangiomas preferentially occurring in bone and penis is characterized by increased cellularity and often worrisome radiologic features. These "cellular" epithelioid hemangiomas are multifocal in 25% of cases, show less vasoformative features and instead a more prominent solid, sheet-like architecture, making their distinction from malignant vascular neoplasms difficult in some instances. Recurrent t(19;19)(q13.2;q13.2) or interstitial del19(q13.2-3) resulting in *ZFP36-FOSB* gene fusion as well as alternate t(3;19)(q25;q12) resulting in *WWTR1-FOSB* gene fusion have been identified in around 20% of cases.[23] Another subset of both conventional and cellular epithelioid hemangiomas (up to 20%) harbors *FOS* rearrangement, resulting from t(1;14)(q22;q24), t(10;14)(p13;q24), or t(3;14)(q25;q24).[24,25]

Epithelioid hemangioma shows universal expression of vascular markers such as CD31 or ERG. In addition, underlying *FOSB* rearrangement can be inferred by diffuse nuclear expression of FOSB by immunohistochemistry (Fig. 2H) in about half of cases.[22] As outlined above, FOSB expression is also observed in most pseudomyogenic hemangioendotheliomas and is therefore not tumor-specific. However, clinical presentation, tumor site, and disparate morphologic appearances are sufficient for a clear diagnostic distinction between these two entities.

THE BIOLOGIC SPECTRUM OF SMARCB1-DEFICIENT TUMORS

An increasing number of biologically unrelated benign and malignant mesenchymal tumors (and rare carcinomas) exhibit loss of SMARCB1 (INI1) expression (Table 1), and in certain instances, the differential diagnosis of a SMARCB1-deficient epithelioid neoplasm may be challenging, especially when evaluating small biopsies.

Malignant rhabdoid tumor is the prototypical malignant neoplasm defined by genomic inactivation of

SMARCB1 on 22q11.23, either by mutations and/or deletions, and associated loss of SMARCB1 expression in tumor cells.[26] Epithelioid sarcoma is another neoplasm in which genomic *SMARCB1* inactivation is observed in the vast majority of cases, either through homozygous deletion or upregulation of miR-206, miR-381, and 671-5p, with associated loss of SMARCB1 expression in around 90% of cases.[27] In addition, SMARCB1 deficiency is found in 10% to 40% of myoepithelial tumors (mostly in pediatric patients)[27] and in 17% of extraskeletal myxoid chondrosarcomas, classically harboring *NR4A3* rearrangement,[27] although the genomic mechanisms leading to SMARCB1 loss remain to be identified in this tumor type. In addition, nearly all renal medullary carcinomas, a highly aggressive renal neoplasm occurring in young patients with sickle cell trait or disease,[28] show SMARCB1 loss resulting from a balanced translocation disrupting *SMARCB1*.[29]

More recently, epithelioid schwannoma, epithelioid MPNST, and poorly differentiated chordoma have been added to the list of SMARCB1-deficient neoplasms and will be discussed in more detail.

Epithelioid Schwannoma

These tumors constitute a rare variant of schwannoma, occur over a wide age range from 13 to 75 years with a mean age of 45 years with an equal sex distribution, and are generally not associated with neurofibromatosis type 1 (NF1) or 2.[30] Most epithelioid schwannomas arise in the limbs and trunk, where they are usually superficially located, but may also rarely be found at visceral locations. Histologically, the tumors show a multilobular architecture and consist of uniform cells with round vesicular nuclei and abundant palely eosinophilic cytoplasm, arranged in sheets or singly dispersed within a myxoid to hyalinized stroma (Fig. 3A). Nuclear pleomorphism, hyperchromasia, and an increased mitotic rate are usually absent. The presence of atypical nuclei has been described in rare cases with malignant transformation to epithelioid MPNST.[30]

Immunohistochemical staining demonstrates diffuse positivity for S100 protein (Fig. 3B) and SOX10 in all cases, as well as expression of glial fibrillary acidic protein in around 40% of cases. Loss of SMARCB1 expression is identified in 42% of epithelioid schwannomas (Fig. 3C).[30]

Although malignant transformation and local recurrences have been described in rare cases, metastatic spread has not been reported.[30]

Epithelioid Malignant Peripheral Nerve Sheath Tumor

In contrast to conventional MPNST which arises in association with NF1 in about half of cases, epithelioid MPNST generally does not occur in a background of NF1.[31] Epithelioid MPNST affects patients over a wide age range from 6 to 80 years with a mean age of 44 years and relatively equal distribution among women and men.[31] The most common site is the lower limb followed by the trunk, and most tumors are superficially located. Like epithelioid schwannoma, epithelioid MPNST shows a multilobular growth pattern and is comprised of epithelioid tumor cells with round, vesicular nuclei and abundant amphophilic to palely eosinophilic cytoplasm, arranged in sheets or nests surrounded by myxoid or fibrous stroma (Fig. 3D). High cellularity and marked nuclear atypia, as well as a high mitotic rate and foci of necrosis distinguish epithelioid MPNST from epithelioid schwannoma.

Expression of S100 protein is strong and diffuse in around 90% of cases (Fig. 3E), to a degree that is unusual for conventional MPNST, which usually shows limited expression in the 40% of cases in which staining is detected.[31] Glial fibrillary acidic protein is positive in 60% of cases, whereas melanocytic markers (eg, melan A, HMB45, and MiTF) are negative. Loss of SMARCB1 expression is found in 67% of epithelioid MPNST (Fig. 3F).

Epithelioid MPNST appears to show a relatively low risk of disease progression—independent of anatomic site or depth—with local recurrences reported in around 30% of cases and distant metastases in 17% of cases.[31]

Poorly Differentiated Chordoma

A rare aggressive variant of chordoma, poorly differentiated chordoma occurs in the skull base/clivus, cervical spine, and sacrum/coccyx of children and young adults between 1 and 29 years with a mean age of 11 years.[32] Histologically, poorly differentiated chordoma bears little resemblance to conventional chordoma and consists of sheets of atypical epithelioid cells with nuclear atypia, abundant eosinophilic cytoplasm, and frequent mitoses (Fig. 3G).[32] Diffuse nuclear expression of the transcription factor brachyury is found in all cases (Fig. 3H), as is staining for keratins. Poorly differentiated chordoma shows consistent loss of SMARCB1 expression (Fig. 3I).

This tumor type follows an aggressive clinical course with a mean overall survival of only 53 months, compared with 109 months for conventional chordoma, and requires aggressive multimodality treatment.[32]

Despite sharing common SMARCB1 deficiency, epithelioid schwannoma, epithelioid MPNST, and poorly differentiated chordoma represent neoplasms that differ substantially in terms of clinical behavior and prognosis, highlighting the importance of correctly diagnosing the various types of epithelioid neoplasms with SMARCB1 loss for optimal patient management.

EMERGING SUBTYPES OF ADIPOCYTIC TUMORS

The diagnostic spectrum of adipocytic tumors with spindle cell features includes spindle cell/pleomorphic lipoma, atypical spindle cell lipomatous tumor, and conventional atypical lipomatous tumor (ALT)/well-differentiated liposarcoma, and, due to overlapping morphologic appearances, correct classification of tumors in this group may be challenging (Table 1).

Spindle Cell/Pleomorphic Lipoma

These tumors are benign adipocytic neoplasms that mostly present as a circumscribed subcutaneous mass in the neck and upper back of middle-aged men. Spindle cell/pleomorphic lipoma is comprised of a bland uniform spindle cell population with an admixed variably prominent component of mature fat. The tumor cells exhibit characteristic short "stubby" nuclei, lack nuclear atypia or pleomorphism, and are embedded in a variably myxoid stroma, often with prominent "ropey" collagen bundles and scattered mast cells (Fig. 4A). The tumor cells in spindle cell/pleomorphic lipoma typically show expression of CD34[33] (Fig. 4B) and loss of nuclear RB1 (Fig. 4C) in most cases, resulting from genomic inactivation of *RB1* at 13q14,[34] which is also a typical feature of cellular angiofibroma and (mammary

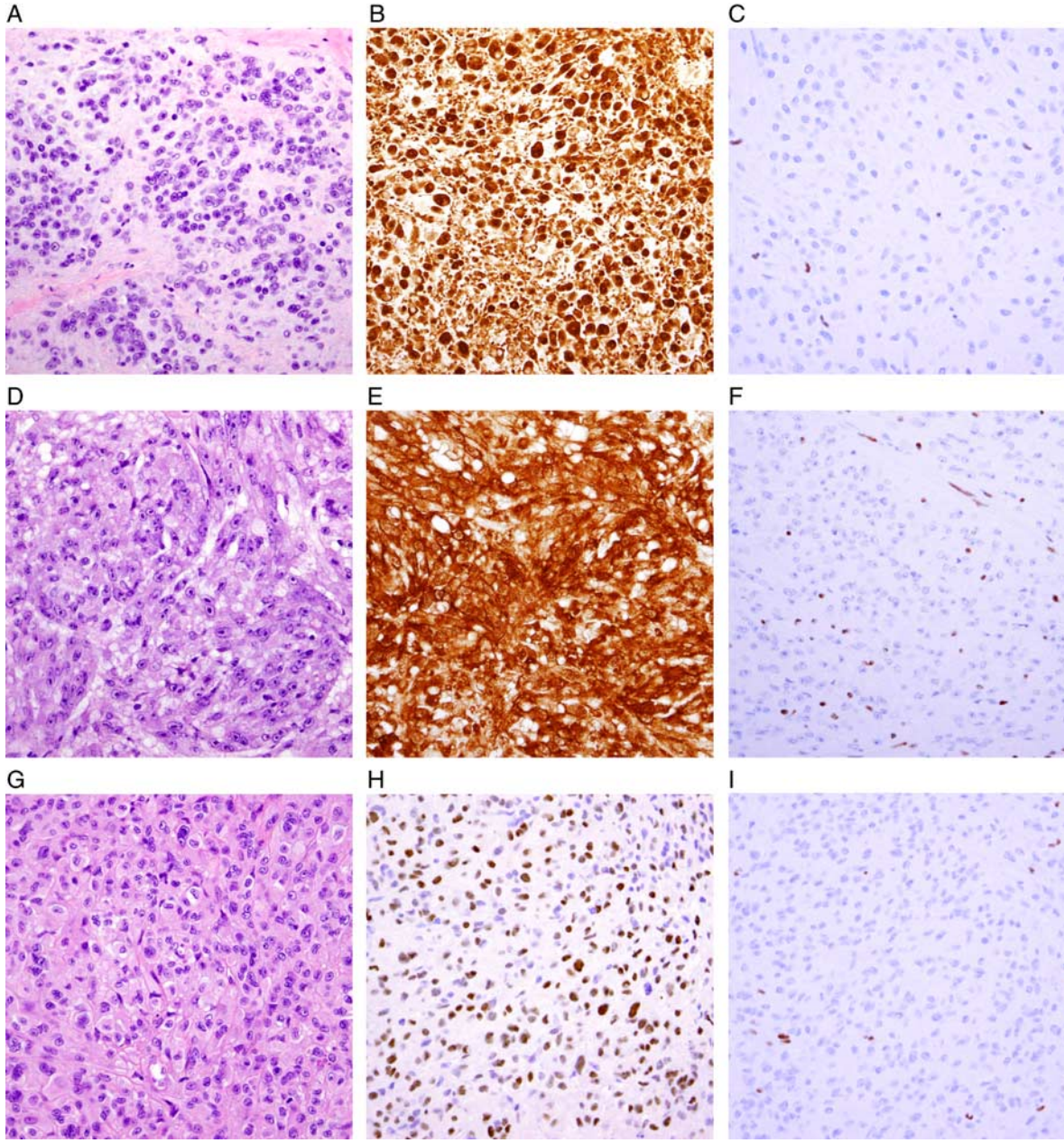

FIGURE 3. The biological spectrum of SMARCB1-deficient tumors. Epithelioid schwannoma is comprised of uniform epithelioid cells with round vesicular nuclei and abundant palely eosinophilic cytoplasm, arranged in sheets or singly dispersed within a myxoid to hyalinized stroma (A). The tumor cells are strongly positivity for S100 protein (B), and a subset of epithelioid schwannomas shows loss of SMARCB1 expression in tumor cells (C); endothelial and inflammatory cells serve as internal control. Epithelioid MPNST is characterized by atypical epithelioid tumor cells with round vesicular nuclei in a lobular or nested growth pattern (D) which, like epithelioid schwannoma, typically exhibit strong and diffuse S100 protein staining (E) to a degree that is rare for conventional MPNST. Most epithelioid MPNST lacks SMARCB1 expression (F). Poorly differentiated chordoma is comprised of epithelioid cells growing in sheets with nuclear atypia and abundant eosinophilic cytoplasm (G). The tumor cells show nuclear expression of the transcription factor brachyury (H) and loss of SMARCB1 expression (I). MPNST indicates malignant peripheral nerve sheath tumor.

type) myofibroblastoma; many experts believe these tumor types are related.

Atypical Spindle Cell Lipomatous Tumor

Over the past few decades, it has become clear that there exists a group of adipocytic neoplasms that do not fit into existing diagnostic categories; such tumors have been variably referred to as "atypical spindle cell lipomatous tumor,"[35] "fibrosarcoma-like lipomatous neoplasm,"[36] and "atypical spindle cell lipoma."[37] Atypical spindle cell lipomatous tumor is a low-grade neoplasm that shows a wide age distribution ranging from 6 to 87 years with a mean age of 54 years and a male predominance. Most cases occur in the limbs and limb girdle, followed by the hands and feet,

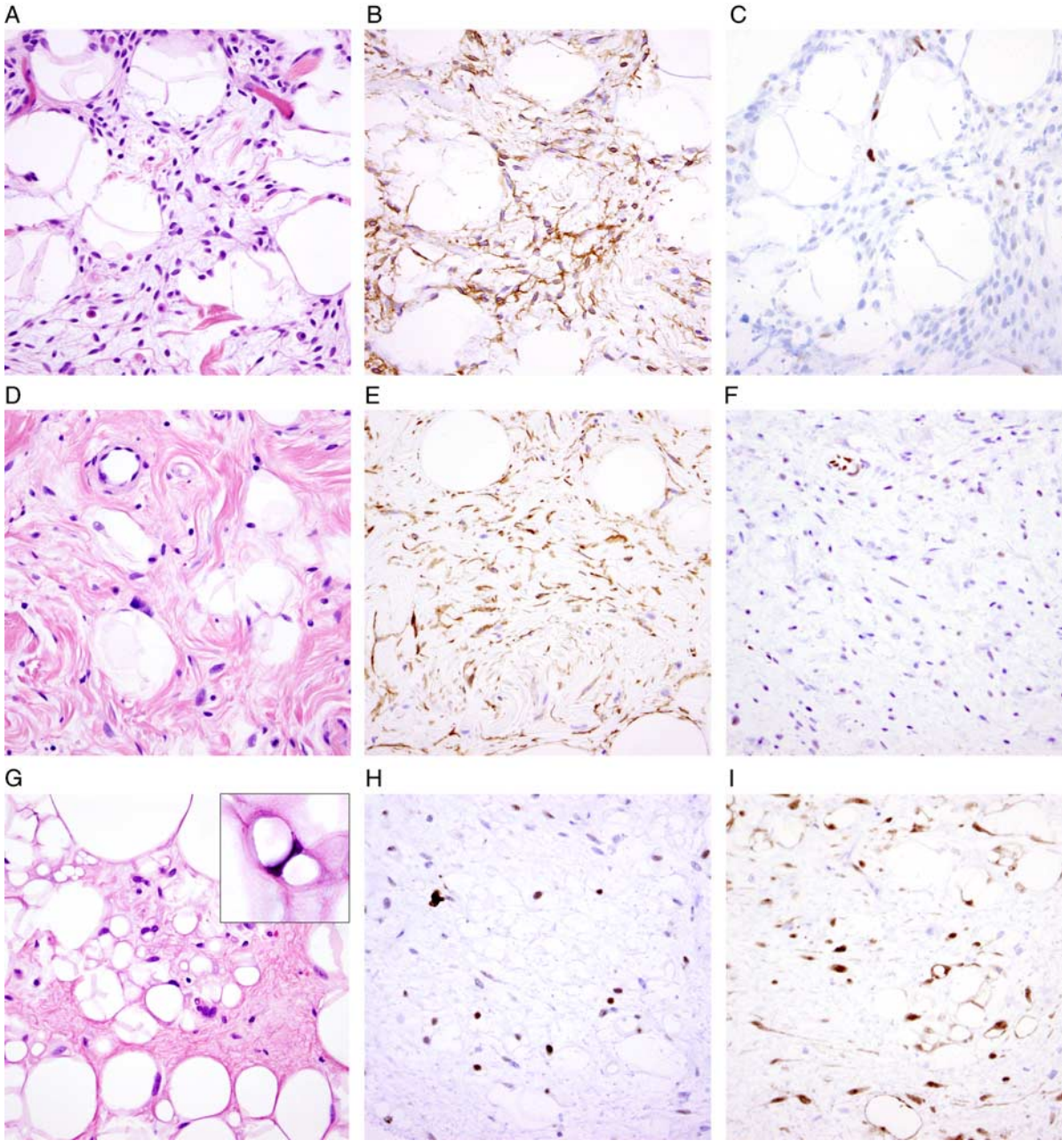

FIGURE 4. Adipocytic tumors with spindle cell morphology. Spindle cell lipoma is comprised of a mature adipocytic component and a bland spindle cell population with characteristic short "stubby" nuclei without atypia, embedded in a variably myxoid to collagenous background often with prominent ropey collagen bundles and admixed mast cells (A). Spindle cell lipomas usually express CD34 (B), and most cases show loss of RB1 expression (C), resulting from genomic inactivation of *RB1* on chromosome 13q14. Atypical spindle cell lipomatous tumor is comprised of mildly atypical spindle cells embedded in a collagenous to myxoid stroma, with focal nuclear atypia (D). As in spindle cell lipoma, ropey collagen bundles and scattered mast cells are often present. Atypical spindle cell lipomatous tumor also shows expression of CD34 (E) and loss of RB1 (F) in many cases. Conventional atypical lipomatous tumor is composed of an adipocytic proliferation with variation in adipocyte size and focal nuclear atypia and hyperchromasia in adipocytes and/or stromal cells (G). Lipoblasts may be present (G, inset) but are not required for the diagnosis. The tumor cells show nuclear expression of MDM2 (H) and CDK4 (I), resulting from high-level chromosome 12q13-15 amplification.

occurring at both superficial and deep locations.[38] Most atypical spindle cell lipomatous tumors are poorly circumscribed with infiltrative margins. The tumors show a wide spectrum of histologic appearances and are characterized by mildly atypical spindle cells in a fibrous or fibromyxoid stroma and a variably prominent adipocytic component with variation in adipocyte size and scattered nuclear atypia (Fig. 4D). Univacuolated or multivacuolated lipoblasts are often present. The immunophenotype is somewhat similar to that of spindle cell/pleomorphic lipoma, including

expression of CD34 in 64% of cases (Fig. 4E), S100 protein in 40%, and, less commonly, desmin (23%). Loss of RB1 expression is found in about half of cases (Fig. 4F). Of note, MDM2 and CDK4 are not overexpressed, and these tumors lack high-level amplification of *MDM2*, which is an important finding in the distinction from conventional ALT. Although atypical spindle cell lipomatous tumors may recur locally in around 10% of cases, they are not associated with dedifferentiation or distant metastasis.[38]

Atypical Lipomatous Tumor

ALT (termed "well-differentiated liposarcoma" when occurring at deep, central body cavity locations, not amenable to complete surgical excision) frequently occurs in the extremities of middle-aged adults and is divided into adipocytic, sclerosing, inflammatory, and spindle cell subtypes.[39,40] Histologically, ALT comprises a mature adipocytic proliferation (to varying extent, depending on histologic subtype) with variation in adipocyte size, and contains atypical adipocytes and stromal cells, which are often enriched in fibrous septa (Fig. 4G). Univacuolated or multivacuolated lipoblasts may be present but are not a requirement for the diagnosis. ALT harbors giant marker or ring chromosomes that contain amplified material from 12q13-15 including the *MDM2*, *CDK4*, and *HMGA2* loci,[41,42] which leads to overexpression of MDM2 (Fig. 4H), CDK4 (Fig. 4I), and HMGA2 by immunohistochemistry.[43]

Spindle cell features are found in rare cases of conventional ALT, overlapping morphologically with atypical spindle cell lipomatous tumor. However, in contrast to atypical spindle cell lipomatous tumor, ALT with spindle cell features shows consistent expression of MDM2 and CDK4 and retained expression of RB1.

MUTATION-SPECIFIC IMMUNOHISTOCHEMISTRY IN THE DIAGNOSIS OF GIANT CELL-RICH BONE TUMORS

The differential diagnosis of giant cell-rich bone tumors comprises a broad spectrum of entities that includes giant cell tumor of bone, chondroblastoma, aneurysmal bone cyst, and osteosarcoma—with substantial differences in biological behavior and clinical management. Although information about patient age, anatomic location of the tumor, and radiologic impression is very important in the diagnostic workup of bone tumors and often helps narrow the differential diagnosis, certain cases with unusual clinical presentation may be diagnostically challenging, especially in small biopsy specimens.

The recent discovery of highly recurrent oncogenic mutations in the *H3F3A* and *H3F3B* genes in subsets of giant cell-rich bone tumors has provided important insights into the genetic underpinnings of these rare bone tumors and has led to the introduction of novel markers that aid in their diagnostic workup (Table 1).[44–49] Of note, *H3F3A* and *H3F3B* are located on different chromosomes but encode histone 3.3 (H3.3) proteins of identical amino acid sequence; oncogenic mutations in these genes are mutually exclusive.

Giant Cell Tumor of Bone

Giant cell tumor of bone most frequently arises in young adults with a mature skeleton and usually develops in the epiphysis of long bones. Malignant transformation is rare but distant metastasis is observed in up to 10% of cases. Histologically, the tumor contains an admixture of ovoid to spindly mononuclear tumor cells, non-neoplastic mononuclear cells, and numerous reactive osteoclast-like giant cells (Fig. 5A).

Approximately 92% of giant cell tumors of bone harbor *H3F3A* (and, rarely, *H3F3B*) mutations, which target codon 34 of H3.3.[44] G34W is the most frequent type of mutation, found in around 85% of cases, followed by alternate G34V, G34R, G34M, or G34L mutations.[44,45,50,51] A mutation-specific antibody directed against mutant H3G34W demonstrates high specificity and sensitivity for the diagnosis of giant cell tumor of bone using immunohistochemistry (Fig. 5B); diffuse nuclear staining is observed in 91% of cases, but not in other giant cell-rich bone tumors.[45] In contrast, staining for H3K36M (see below) is negative in giant cell tumor of bone (Fig. 5C).

As the mutation-specific H3G34W antibody fails to detect alternate mutations involving codon 34, negative H3G34W immunohistochemistry does not preclude the diagnosis of giant cell tumor of bone; additional antibodies specifically directed at other amino acid exchanges at codon 34 may be helpful.[50] Alternatively, genomic sequencing may be performed to detect an underlying mutation; reported detection rates range from 69% for Sanger sequencing[47] to 96% for targeted next-generation sequencing.[48] However, such studies are rarely needed in clinical practice, since the combination of histologic and radiologic features is usually sufficient for diagnosis. Of note, previous denosumab treatment, decalcification, and malignant transformation do not significantly affect the results obtained by immunohistochemistry or sequencing.

Chondroblastoma

Chondroblastoma affects mostly children and adolescents with an immature skeleton and usually involves the epiphysis of long bones, with or without extension to the articular cartilage. Histologically, chondroblastoma is comprised of mononuclear cells and admixed multinucleated giant cells embedded in a dense eosinophilic matrix (Fig. 5D). Occasionally, characteristic "chicken-wire" calcification is observed.

In contrast to giant cell tumor of bone, chondroblastoma lacks H3G34W expression (Fig. 5E). Instead, this tumor is characterized by oncogenic *H3F3B* (and, rarely, *H3F3A*) mutations that encode H3.3 K36M, which can be detected by sequencing in 70% to 100% of cases, depending on the method used.[44,47–49,52] A mutation-specific H3K36M antibody demonstrates diffuse nuclear expression in 96% of chondroblastomas by immunohistochemistry (Fig. 5F) but not in histologic mimics.[46]

The high specificity of H3G34W and H3K36M immunohistochemistry in the diagnosis of giant cell tumor of bone and chondroblastoma, respectively, highlights the value of these markers in the often challenging differential diagnosis of bone tumors, especially when only limited biopsy material is available.[51] However, it is important to emphasize that the heterozygous oncogenic *H3F3A* and *H3F3B* mutations are restricted to the neoplastic mononuclear cells, often accounting for <50% of cells. The relatively low mutant allele fraction of around 25% may therefore lead to false-negative results when Sanger sequencing is performed;[47,51] careful correlation between radiologic and morphologic features is required.

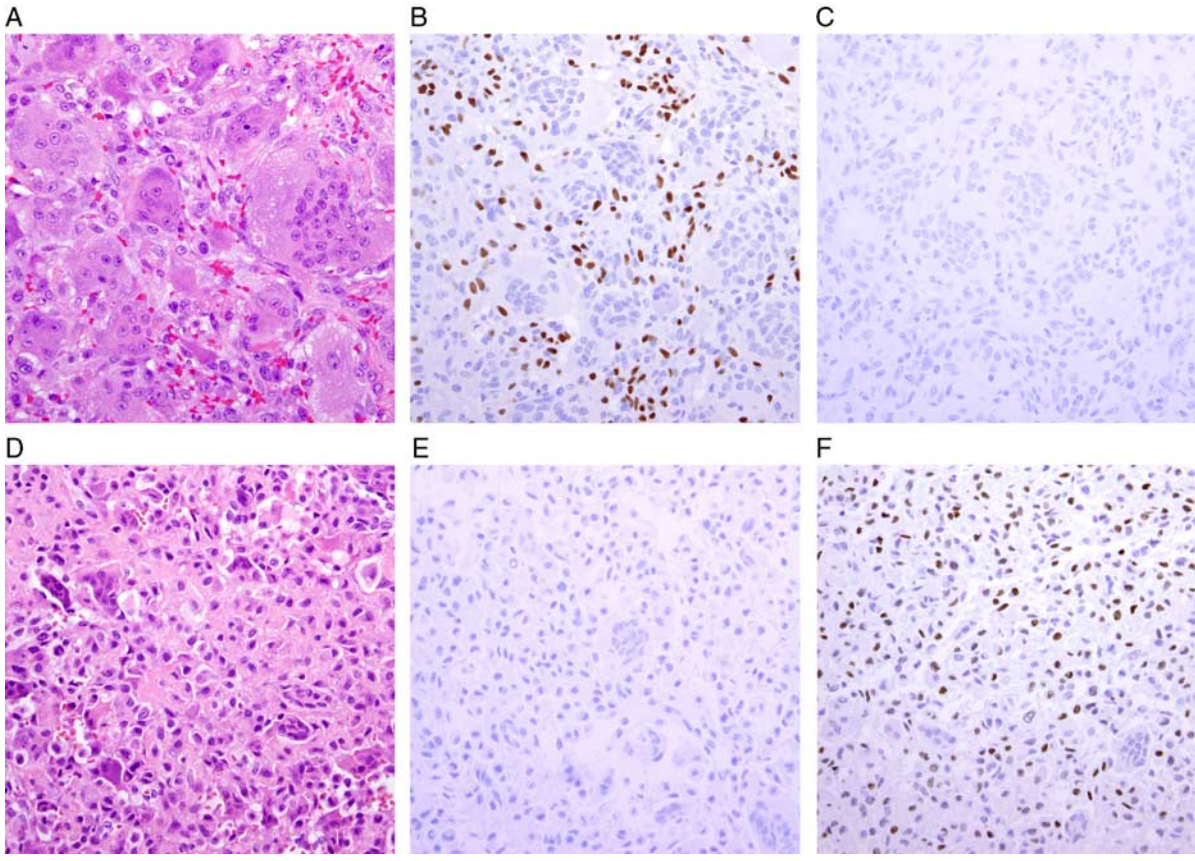

FIGURE 5. Mutation-specific immunohistochemistry in the diagnosis of giant cell-rich bone tumors. Giant cell tumor of bone is comprised of ovoid to spindled mononuclear tumor cells with numerous admixed non-neoplastic multinucleated osteoclast-like giant cells (A). Mutation-specific immunohistochemistry for H3G34W encoded by mutant *H3F3A* (or, less frequently, *H3F3B*) shows diffuse nuclear expression in tumor cells in most cases (B), whereas staining for H3K36M is negative (C). Chondroblastoma is comprised of mononuclear cells and admixed multinucleated giant cells embedded in a dense eosinophilic matrix (D). Mutation-specific immunohistochemistry for H3G34W is negative (E), whereas staining for H3K36M, encoded by mutant *H3F3B* (or, less frequently, *H3F3A*), shows diffuse nuclear staining in tumor cells (F). Note that admixed giant cells are non-neoplastic in giant cell tumor of bone and chondroblastoma and stain negative for H3G34W and H3K36M.

BIPHENOTYPIC SINONASAL SARCOMA SHOWS CHARACTERISTIC IMMUNOPHENOTYPIC AND CYTOGENETIC FEATURES

Biphenotypic sinonasal sarcoma—a low-grade spindle cell sarcoma arising in the upper sinonasal tract of middle-aged adults—was initially described in 2012 by Lewis et al[53], including two cases with identical t(2;4). Biphenotypic sinonasal sarcoma is defined by characteristic co-expression of neural and myogenic markers, and, as discovered more recently, harbors recurrent *PAX3* rearrangement, with *PAX3-MAML3* fusion resulting from t(2;4)(q35;q31) being most frequent,[54,55] followed by alternate *PAX3-FOXO1*[56] or *PAX3-NCOA1*[57] fusions.

Histologically, biphenotypic sinonasal sarcoma is comprised of a homogeneously cellular spindle cell population arranged in short fascicles (Fig. 6A). The tumor cells show bland elongated nuclei and scant cytoplasm without significant nuclear atypia or pleomorphism. Necrosis and mitotic figures are uncommon. Concomitant neural and myogenic differentiation is reflected by its immunophenotype (Table 1): co-expression of S100 protein (Fig. 6B) and SMA (Fig. 6C) or calponin, and, less commonly, desmin and myogenin (the latter only in rare cells), is characteristic of biphenotypic sinonasal sarcoma; a subset of cases also expresses TLE1. In addition, most biphenotypic sinonasal sarcomas show nuclear expression of β-catenin, whereas SOX10 is negative.[58]

The differential diagnosis of biphenotypic sinonasal sarcoma includes other spindle cell sarcomas, chiefly low-grade MPNST and monophasic synovial sarcoma, which rarely occur in this anatomic location. Before its recognition as a distinct entity, most cases of biphenotypic sinonasal sarcoma were presumably diagnosed as either MPNST or synovial sarcoma based on morphologic and immunophenotypic similarities. In contrast to MPNST, biphenotypic sinonasal sarcoma lacks alternation of hypercellular and hypocellular areas and accentuation of tumor cells around blood vessels. Prominent hemangiopericytoma-like blood vessels—which are often found in synovial sarcomas—may sometimes be observed. Of note, the immunophenotype of biphenotypic sinonasal sarcoma is not tumor-specific and may pose diagnostic challenges: cases with positive staining for TLE1 may be confused with synovial sarcoma; a subset of MPNST also show expression of TLE1. Expression of S100 protein is not only a feature of biphenotypic sinonasal sarcoma but can also be found in up to 40% of MPNST

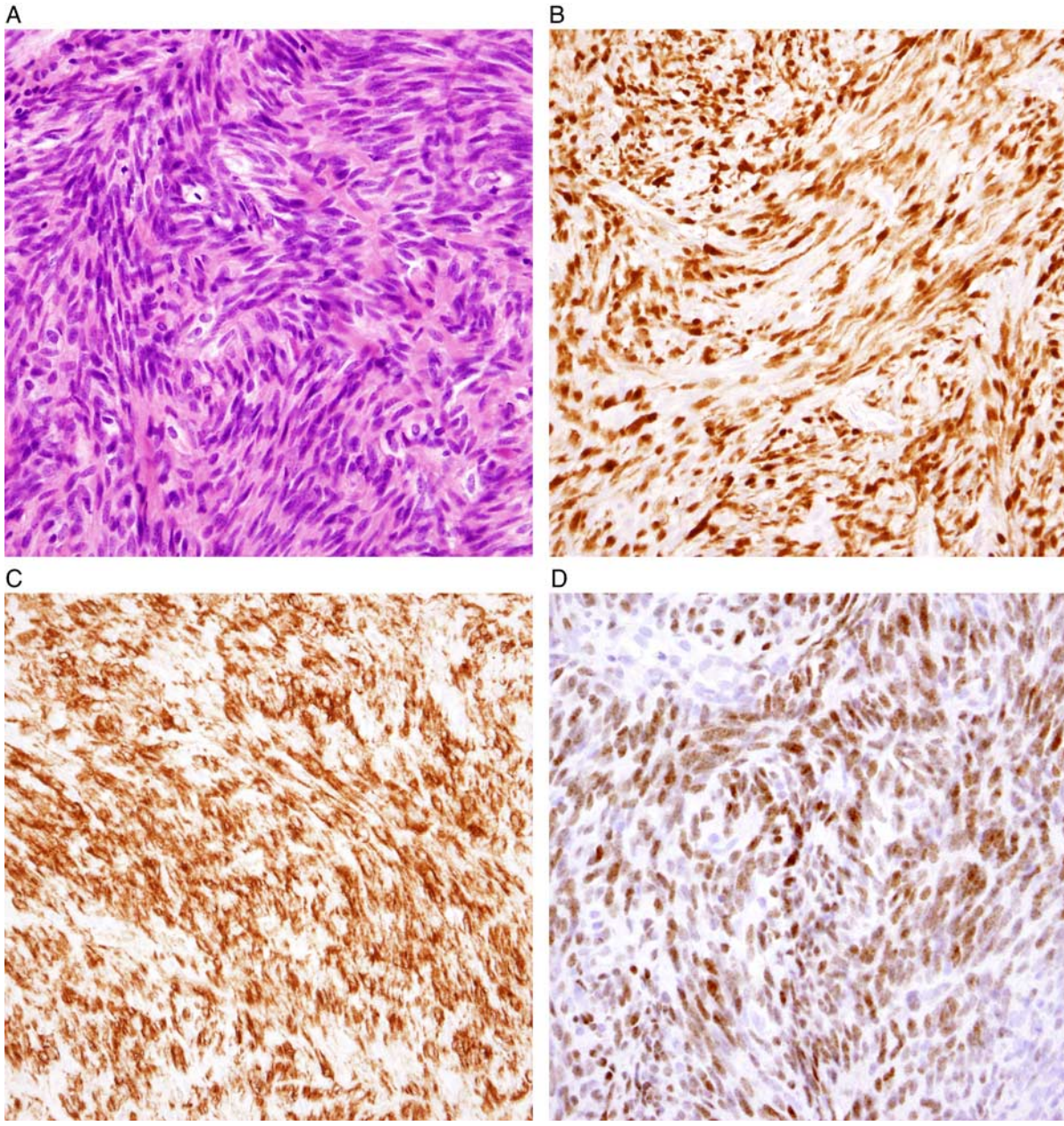

FIGURE 6. Biphenotypic sinonasal sarcoma with characteristic immunophenotypic and cytogenetic features. Biphenotypic sinonasal sarcoma is a low-grade sarcoma composed of cellular fascicles of uniform spindle cells with bland elongated nuclei and scant cytoplasm (A). The tumor cells show characteristic co-expression of S100 protein (B) and myogenic markers, such as SMA (C). Nuclear expression of PAX3, resulting from *PAX3* rearrangement, is detected in most cases (D).

(usually limited in extent, however) and up to 30% of synovial sarcomas.[56] Likewise, absence of SOX10 expression does not aid in the distinction from MPNST, which is negative for this marker in more than half of cases.

A recent study evaluated PAX3 expression in biphenotypic sinonasal sarcoma and demonstrated positive staining in all cases tested. Histologic mimics were largely negative, except for 1 case (10%) of spindle cell rhabdomyosarcoma; alveolar rhabdomyosarcomas were also positive (80%), as might be expected from underlying *PAX3* gene rearrangement. The high sensitivity of 100% and specificity of 98% suggest that PAX3 may serve as a helpful diagnostic marker in this context.[59] Of note, due to cross-reactivity with PAX3, biphenotypic sinonasal sarcomas also show positive staining with polyclonal PAX8 antibodies in most cases.[59]

As demonstrated in a large study of 44 cases, biphenotypic sinonasal sarcomas harbor *PAX3-MAML3* fusion in 55% of cases, and less frequently, alternate *PAX3-FOXO1* or *PAX3-NCOA1* fusion.[55] Rare cases show *MAML3* rearrangement with an unknown fusion partner or lack a detectable structural rearrangement.[55] These findings suggest that absence of *PAX3* rearrangement (and concurrent PAX3 expression) do not necessarily rule out a

diagnosis of biphenotypic sinonasal sarcoma; correlation of clinical presentation with morphologic appearances and immunophenotype remains important in such cases.

Despite bearing the same *PAX3-FOXO1* fusion as a subset of alveolar rhabdomyosarcomas, biphenotypic sinonasal sarcoma is considered a low-grade sarcoma that may show locally aggressive behavior but rarely metastasizes.

CONCLUSIONS

The integrated use of conventional cytogenetics, targeted next-generation sequencing, and immunohistochemistry has led to marked improvements in the diagnostic workup of soft tissue tumors in recent years. Advances in the diagnosis of round cell sarcomas have led to the introduction of *CIC*-rearranged and *BCOR*-rearranged sarcomas as entities distinct from Ewing sarcoma into current classification systems. In addition, identification of specific cytogenetic alterations in vascular tumors distinguishes subtypes within the groups of epithelioid hemangioendothelioma and epithelioid hemangioma, and identified a characteristic aberration in pseudomyogenic hemangioendothelioma. However, many immunohistochemical markers that relate to an underlying genomic alteration are not completely tumor specific and need to be interpreted with caution, but are nonetheless more sensitive and specific than conventional lineage-associated markers. SMARCB1 deficiency is observed in a diverse range of neoplasms but may—in conjunction with tumor site, presentation, and other immunohistochemical markers—be of substantial diagnostic value. Existing immunohistochemical stains in the group of adipocytic neoplasms further help separate the recently described atypical spindle cell lipomatous tumor from conventional ALT. The recent discovery of highly recurrent oncogenic *H3F3A* and *H3F3B* mutations that define giant cell tumor of bone and chondroblastoma, respectively, prompted the introduction of highly sensitive mutation-specific antibodies that provide additional insights into the oncogenic mechanisms that drive these rare benign bone tumors. Finally, biphenotypic sinonasal sarcoma sets an example of how the recognition of a unique immunophenotype, identification of *PAX3* rearrangement and PAX3 expression helped delineate a novel diagnostic entity.

Nonetheless, the careful integration of all available information and critical interpretation of established and novel diagnostic markers remains crucial in the diagnosis of soft tissue tumors.

ACKNOWLEDGMENT

The authors thank Dr Christopher D.M. Fletcher, Department of Pathology, Brigham and Women's Hospital, Harvard Medical School, for contributing some of the cases illustrated.

REFERENCES

1. Folpe AL, Goldblum JR, Rubin BP, et al. Morphologic and immunophenotypic diversity in Ewing family tumors: a study of 66 genetically confirmed cases. *Am J Surg Pathol*. 2005;29:1025–1033.
2. Hung YP, Fletcher CD, Hornick JL. Evaluation of NKX2-2 expression in round cell sarcomas and other tumors with EWSR1 rearrangement: imperfect specificity for Ewing sarcoma. *Mod Pathol*. 2016;29:370–380.
3. Yoshida A, Sekine S, Tsuta K, et al. NKX2.2 is a useful immunohistochemical marker for Ewing sarcoma. *Am J Surg Pathol*. 2012;36:993–999.
4. Shibuya R, Matsuyama A, Nakamoto M, et al. The combination of CD99 and NKX2.2, a transcriptional target of EWSR1-FLI1, is highly specific for the diagnosis of Ewing sarcoma. *Virchows Arch*. 2014;465:599–605.
5. Sugita S, Arai Y, Tonooka A, et al. A novel CIC-FOXO4 gene fusion in undifferentiated small round cell sarcoma: a genetically distinct variant of Ewing-like sarcoma. *Am J Surg Pathol*. 2014;38:1571–1576.
6. Solomon DA, Brohl AS, Khan J, et al. Clinicopathologic features of a second patient with Ewing-like sarcoma harboring CIC-FOXO4 gene fusion. *Am J Surg Pathol*. 2014;38:1724–1725.
7. Italiano A, Sung YS, Zhang L, et al. High prevalence of CIC fusion with double-homeobox (DUX4) transcription factors in EWSR1-negative undifferentiated small blue round cell sarcomas. *Genes Chromosomes Cancer*. 2012;51:207–218.
8. Specht K, Zhang L, Sung YS, et al. Novel BCOR-MAML3 and ZC3H7B-BCOR Gene fusions in undifferentiated small blue round cell sarcomas. *Am J Surg Pathol*. 2016;40:433–442.
9. Antonescu CR, Owosho AA, Zhang L, et al. Sarcomas with CIC-rearrangements are a distinct pathologic entity with aggressive outcome: a clinicopathologic and molecular study of 115 cases. *Am J Surg Pathol*. 2017;41:941–949.
10. Pierron G, Tirode F, Lucchesi C, et al. A new subtype of bone sarcoma defined by BCOR-CCNB3 gene fusion. *Nat Genet*. 2012;44:461–466.
11. Kao YC, Owosho AA, Sung YS, et al. BCOR-CCNB3 fusion positive sarcomas: a clinicopathologic and molecular analysis of 36 cases with comparison to morphologic spectrum and clinical behavior of other round cell sarcomas. *Am J Surg Pathol*. 2018;42:604–615.
12. Cohen-Gogo S, Cellier C, Coindre JM, et al. Ewing-like sarcomas with BCOR-CCNB3 fusion transcript: a clinical, radiological and pathological retrospective study from the Societe Francaise des Cancers de L'Enfant. *Pediatr Blood Cancer*. 2014;61:2191–2198.
13. Kao YC, Sung YS, Zhang L, et al. BCOR overexpression is a highly sensitive marker in round cell sarcomas with BCOR genetic abnormalities. *Am J Surg Pathol*. 2016;40:1670–1678.
14. Fletcher C, Bridge JA, Hogendoorn PCW, et al. *WHO Classification of Tumours of Soft Tissue and Bone*. Lyon: IARC Press; 2013.
15. Mendlick MR, Nelson M, Pickering D, et al. Translocation t (1;3)(p36.3;q25) is a nonrandom aberration in epithelioid hemangioendothelioma. *Am J Surg Pathol*. 2001;25:684–687.
16. Tanas MR, Sboner A, Oliveira AM, et al. Identification of a disease-defining gene fusion in epithelioid hemangioendothelioma. *Sci Transl Med*. 2011;3:98ra82.
17. Errani C, Zhang L, Sung YS, et al. A novel WWTR1-CAMTA1 gene fusion is a consistent abnormality in epithelioid hemangioendothelioma of different anatomic sites. *Genes Chromosomes Cancer*. 2011;50:644–653.
18. Doyle LA, Fletcher CD, Hornick JL. Nuclear expression of CAMTA1 distinguishes epithelioid hemangioendothelioma from histologic mimics. *Am J Surg Pathol*. 2016;40:94–102.
19. Antonescu CR, Le Loarer F, Mosquera JM, et al. Novel YAP1-TFE3 fusion defines a distinct subset of epithelioid hemangioendothelioma. *Genes Chromosomes Cancer*. 2013;52:775–784.
20. Hornick JL, Fletcher CD. Pseudomyogenic hemangioendothelioma: a distinctive, often multicentric tumor with indolent behavior. *Am J Surg Pathol*. 2011;35:190–201.
21. Walther C, Tayebwa J, Lilljebjorn H, et al. A novel SERPINE1-FOSB fusion gene results in transcriptional up-regulation of FOSB in pseudomyogenic haemangioendothelioma. *J Pathol*. 2014;232:534–540.
22. Hung YP, Fletcher CD, Hornick JL. FOSB is a useful diagnostic marker for pseudomyogenic hemangioendothelioma. *Am J Surg Pathol*. 2017;41:596–606.

23. Antonescu CR, Chen HW, Zhang L, et al. ZFP36-FOSB fusion defines a subset of epithelioid hemangioma with atypical features. *Genes Chromosomes Cancer*. 2014;53:951–959.
24. Van Ijzendoorn DG, de Jong D, Romagosa C, et al. Fusion events lead to truncation of FOS in epithelioid hemangioma of bone. *Genes Chromosomes Cancer*. 2015;54:565–574.
25. Huang SC, Zhang L, Sung YS, et al. Frequent FOS gene rearrangements in epithelioid hemangioma: a molecular study of 58 cases with morphologic reappraisal. *Am J Surg Pathol*. 2015;39:1313–1321.
26. Biegel JA, Fogelgren B, Wainwright LM, et al. Germline INI1 mutation in a patient with a central nervous system atypical teratoid tumor and renal rhabdoid tumor. *Genes Chromosomes Cancer*. 2000;28:31–37.
27. Hornick JL, Dal Cin P, Fletcher CD. Loss of INI1 expression is characteristic of both conventional and proximal-type epithelioid sarcoma. *Am J Surg Pathol*. 2009;33:542–550.
28. Davis CJ Jr, Mostofi FK, Sesterhenn IA. Renal medullary carcinoma. The seventh sickle cell nephropathy. *Am J Surg Pathol*. 1995;19:1–11.
29. Calderaro J, Masliah-Planchon J, Richer W, et al. Balanced translocations disrupting SMARCB1 are hallmark recurrent genetic alterations in renal medullary carcinomas. *Eur Urol*. 2016;69:1055–1061.
30. Jo VY, Fletcher CDM. SMARCB1/INI1 loss in epithelioid schwannoma: a clinicopathologic and immunohistochemical study of 65 cases. *Am J Surg Pathol*. 2017;41:1013–1022.
31. Jo VY, Fletcher CD. Epithelioid malignant peripheral nerve sheath tumor: clinicopathologic analysis of 63 cases. *Am J Surg Pathol*. 2015;39:673–682.
32. Shih AR, Cote GM, Chebib I, et al. Clinicopathologic characteristics of poorly differentiated chordoma. *Mod Pathol*. 2018. [In press].
33. Templeton SF, Solomon AR Jr. Spindle cell lipoma is strongly CD34 positive. An immunohistochemical study. *J Cutan Pathol*. 1996;23:546–550.
34. Dal Cin P, Sciot R, Polito P, et al. Lesions of 13q may occur independently of deletion of 16q in spindle cell/pleomorphic lipomas. *Histopathology*. 1997;31:222–225.
35. Mentzel T, Palmedo G, Kuhnen C. Well-differentiated spindle cell liposarcoma ('atypical spindle cell lipomatous tumor') does not belong to the spectrum of atypical lipomatous tumor but has a close relationship to spindle cell lipoma: clinicopathologic, immunohistochemical, and molecular analysis of six cases. *Mod Pathol*. 2010;23:729–736.
36. Deyrup AT, Chibon F, Guillou L, et al. Fibrosarcoma-like lipomatous neoplasm: a reappraisal of so-called spindle cell liposarcoma defining a unique lipomatous tumor unrelated to other liposarcomas. *Am J Surg Pathol*. 2013;37:1373–1378.
37. Creytens D, van Gorp J, Savola S, et al. Atypical spindle cell lipoma: a clinicopathologic, immunohistochemical, and molecular study emphasizing its relationship to classical spindle cell lipoma. *Virchows Arch*. 2014;465:97–108.
38. Marino-Enriquez A, Nascimento AF, Ligon AH, et al. Atypical spindle cell lipomatous tumor: clinicopathologic characterization of 232 cases demonstrating a morphologic spectrum. *Am J Surg Pathol*. 2017;41:234–244.
39. Laurino L, Furlanetto A, Orvieto E, et al. Well-differentiated liposarcoma (atypical lipomatous tumors). *Semin Diagn Pathol*. 2001;18:258–262.
40. Lucas DR, Nascimento AG, Sanjay BK, et al. Well-differentiated liposarcoma. The Mayo Clinic experience with 58 cases. *Am J Clin Pathol*. 1994;102:677–683.
41. Rosai J, Akerman M, Dal Cin P, et al. Combined morphologic and karyotypic study of 59 atypical lipomatous tumors. Evaluation of their relationship and differential diagnosis with other adipose tissue tumors (a report of the CHAMP Study Group). *Am J Surg Pathol*. 1996;20:1182–1189.
42. Italiano A, Bianchini L, Keslair F, et al. HMGA2 is the partner of MDM2 in well-differentiated and dedifferentiated liposarcomas whereas CDK4 belongs to a distinct inconsistent amplicon. *Int J Cancer*. 2008;122:2233–2241.
43. Dei Tos AP, Doglioni C, Piccinin S, et al. Coordinated expression and amplification of the MDM2, CDK4, and HMGI-C genes in atypical lipomatous tumours. *J Pathol*. 2000;190:531–536.
44. Behjati S, Tarpey PS, Presneau N, et al. Distinct H3F3A and H3F3B driver mutations define chondroblastoma and giant cell tumor of bone. *Nat Genet*. 2013;45:1479–1482.
45. Amary F, Berisha F, Ye H, et al. H3F3A (Histone 3.3) G34W immunohistochemistry: a reliable marker defining benign and malignant giant cell tumor of bone. *Am J Surg Pathol*. 2017;41:1059–1068.
46. Amary MF, Berisha F, Mozela R, et al. The H3F3 K36M mutant antibody is a sensitive and specific marker for the diagnosis of chondroblastoma. *Histopathology*. 2016;69:121–127.
47. Cleven AH, Hocker S, Briaire-de Bruijn I, et al. Mutation analysis of H3F3A and H3F3B as a diagnostic tool for giant cell tumor of bone and chondroblastoma. *Am J Surg Pathol*. 2015;39:1576–1583.
48. Presneau N, Baumhoer D, Behjati S, et al. Diagnostic value of H3F3A mutations in giant cell tumour of bone compared to osteoclast-rich mimics. *J Pathol Clin Res*. 2015;1:113–123.
49. Kervarrec T, Collin C, Larousserie F, et al. H3F3 mutation status of giant cell tumors of the bone, chondroblastomas and their mimics: a combined high resolution melting and pyrosequencing approach. *Mod Pathol*. 2017;30:393–406.
50. Yamamoto H, Iwasaki T, Yamada Y, et al. Diagnostic utility of histone H3.3G34 W, G34R, and G34 V mutant-specific antibodies for giant cell tumors of bone. *Hum Pathol*. 2018;73:41–50.
51. Schaefer IM, Fletcher JA, Nielsen GP, et al. Immunohistochemistry for histone H3G34W and H3K36M is highly specific for giant cell tumor of bone and chondroblastoma, respectively, in FNA and core needle biopsy. *Cancer Cytopathol*. 2018. [In press].
52. Nohr E, Lee LH, Cates JM, et al. Diagnostic value of histone 3 mutations in osteoclast-rich bone tumors. *Hum Pathol*. 2017;68:119–127.
53. Lewis JT, Oliveira AM, Nascimento AG, et al. Low-grade sinonasal sarcoma with neural and myogenic features: a clinicopathologic analysis of 28 cases. *Am J Surg Pathol*. 2012;36:517–525.
54. Wang X, Bledsoe KL, Graham RP, et al. Recurrent PAX3-MAML3 fusion in biphenotypic sinonasal sarcoma. *Nat Genet*. 2014;46:666–668.
55. Fritchie KJ, Jin L, Wang X, et al. Fusion gene profile of biphenotypic sinonasal sarcoma: an analysis of 44 cases. *Histopathology*. 2016;69:930–936.
56. Wong WJ, Lauria A, Hornick JL, et al. Alternate PAX3--FOXO1 oncogenic fusion in biphenotypic sinonasal sarcoma. *Genes Chromosomes Cancer*. 2016;55:25–29.
57. Huang SC, Ghossein RA, Bishop JA, et al. Novel PAX3-NCOA1 fusions in biphenotypic sinonasal sarcoma with focal rhabdomyoblastic differentiation. *Am J Surg Pathol*. 2016;40:51–59.
58. Rooper LM, Huang SC, Antonescu CR, et al. Biphenotypic sinonasal sarcoma: an expanded immunoprofile including consistent nuclear beta-catenin positivity and absence of SOX10 expression. *Hum Pathol*. 2016;55:44–50.
59. Jo V, Mariño-Enríquez A, Fletcher CDM, et al. Expression of PAX3 distinguishes biphenotypic sinonasal sarcoma from histologic mimics. *Am J Surg Pathol*. 2018. [In press].